Rb^{85}-Rb^{86} Hyperfine-Structure Anomaly*†

NORMAN BRASLAU,‡ GILBERT O. BRINK, AND JHAN M. KHAN§
Lawrence Radiation Laboratory, University of California, Berkeley, California

(Received April 21, 1961)

The atomic beam magnetic-resonance method with separated oscillatory fields has been used to measure the hyperfine structure separation and magnetic dipole moment of the isotopes Rb^{85} and 18.6-day Rb^{86} in the $^2S_{\frac{1}{2}}$ electronic ground state. Observation of the separation of a $\Delta F=\pm 1$ doublet in the intermediate field region gives the value of the moment; the minimum value of the mean doublet frequency gives the value of $\Delta\nu$. Observation of another $\Delta F=\pm 1$ doublet in low field also yields a value for $\Delta\nu$.

Results obtained for Rb^{85} are in good agreement with previously published values and indicate that transition frequencies calculated from the Breit-Rabi equation agree with experiment to at least one part per million.

For Rb^{86} the following values are obtained for the $^2S_{\frac{1}{2}}$ ground state: $\Delta\nu=3946.883(2)$ Mc/sec, $g_I=-4.590(4)\times 10^{-4}$, and $\mu_I=-1.6856(14)$ nm (without diamagnetic correction).

The hyperfine-structure anomaly arises in part from the difference of the volume distribution of nuclear magnetism in the two nuclei and is defined as the deviation from equality of the ratio of the hyperfine-splitting factors of two isotopes to the ratio of their nuclear g factors. For these two isotopes its value is found to be $^{85}\Delta^{86}=0.17(9)\%$.

The Bohr-Weisskopf theory of the hfs anomaly is applied to these isotopes with calculations based on a single-particle model with varying distributions of spin and orbital contributions to the magnetic moment.

I. INTRODUCTION

IN addition to intrinsic nuclear properties such as spin and multipole moments, measurement of the volume distribution of the magnetic dipole moment has contributed to the development of the theory of nuclear structure. Bitter pointed out that information could be obtained about the distribution of magnetism by the study of hyperfine structure of atoms in which the expectation value of the electronic wave function is nonzero at the position of the nucleus.[1] For heavy nuclei, Bohr and Weisskopf have developed a quantitative theory to explain the effects of volume distribution on hyperfine structure.[2] This theory has been extended by Bohr,[3,4] Eisinger and Jaccarino,[5] and Stroke.[6]

Fermi derived the expression for the hfs splitting factor of a hydrogen-like atom with a point dipole nucleus of spin I and magnetic moment μ_I ($\mu_I=g_I\mu_0 I$) to be

$$a=-(8\pi/3)g_I g_J\mu_0^2|\psi(0)|^2, \tag{1}$$

where

$$a=2h\Delta\nu/(2I+1), \tag{2}$$

and μ_0 is the Bohr magneton, g_J is the electronic g factor, $\psi(0)$ is the electronic wave function at the position of the nucleus, and $\Delta\nu$ is the hyperfine-structure separation.[7] If the magnetism is assumed to be distributed over the finite volume of the nucleus, the hfs interaction would be expected to be reduced by a small amount ϵ from that calculated for a point dipole. Since the atomic wave functions for heavy nuclei are not well known, one can compare ratios of the hfs interaction in two isotopes and eliminate the uncertainty in the contribution of the wave functions. For a point dipole (PD), from Eqs. (1) and (2),

$$\left(\frac{\Delta\nu_1}{\Delta\nu_2}\right)_{\rm PD}=\frac{g_{I1}}{g_{I2}}\frac{(2I_1+1)}{(2I_2+1)}, \tag{3}$$

whereas for a nucleus of finite size, where $\Delta\nu$ is taken to be the experimental value,

$$\frac{\Delta\nu_1}{\Delta\nu_2}=\left(\frac{\Delta\nu_1}{\Delta\nu_2}\right)_{\rm PD}\frac{(1+\epsilon_1)}{(1+\epsilon_2)}, \tag{4}$$

so that

$$\frac{\Delta\nu_1}{\Delta\nu_2}=\frac{g_{I1}}{g_{I2}}\left(\frac{2I_1+1}{2I_2+1}\right)(1+{}^1\Delta^2), \tag{5}$$

where, neglecting terms of order ϵ^2, the hfs anomaly is

$${}^1\Delta^2\equiv\epsilon_1-\epsilon_2. \tag{6}$$

With a few exceptions, anomalies have been measured on pairs of stable isotopes, where the $\Delta\nu$'s are usually measured by atomic beam methods and the moment ratio by NMR techniques. It would be most interesting to measure the anomalies in a series of adjacent isotopes where the effect of adding one neutron after another can be investigated. Eisinger, Bederson, and Feld, in their measurement of the K^{39}-K^{40} anomaly, showed that the moment could be measured directly by atomic beam techniques.[8] The detection of trace amounts of isotopes in a beam by mass spectrometer was employed by

* This work was supported in part by the U. S. Atomic Energy Commission and in part by the National Science Foundation.

† From a thesis submitted by N. Braslau in partial fulfillment of the requirements for the degree of Doctor of Philosophy at the University of California.

‡ Present address: Ecole Normale Superieure, Rue Lhomond, Paris 5, France.

§ Present address: Cavendish Laboratory, Free School Lane, Cambridge, England.

[1] F. Bitter, Phys. Rev. **76**, 150 (1949).

[2] A. Bohr and V. Weisskopf, Phys. Rev. **77**, 94 (1950).

[3] A. Bohr, Phys. Rev. **81**, 134 (1951).

[4] A. Bohr, Phys. Rev. **81**, 331 (1951).

[5] J. Eisinger and V. Jaccarino, Revs. Modern Phys. **30**, 528 (1958). This is a review article covering the subject of the distribution of nuclear magnetism to that date.

[6] H. H. Stroke, Quarterly Progress Report No. 54, Research Laboratory of Electronics, Massachusetts Institute of Technology, July 15, 1959 (unpublished).

[7] E. Fermi, Z. Physik **60**, 320 (1930).

[8] J. Eisinger, B. Bederson, and B. T. Feld, Phys. Rev. **86**, 73 (1952).

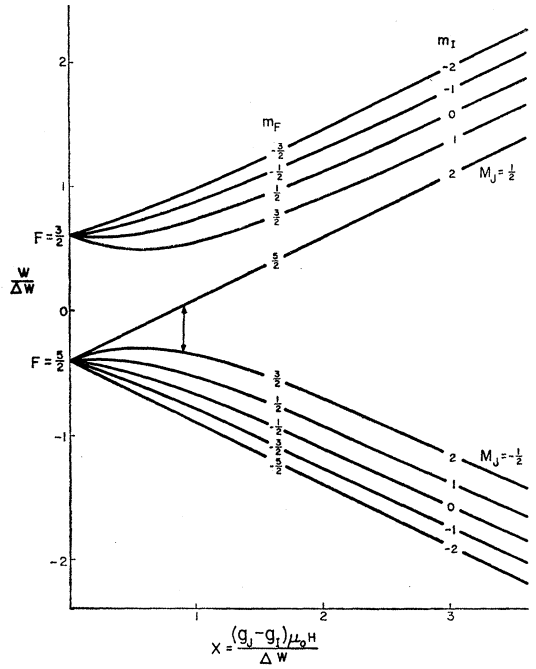

FIG. 1. Breit-Rabi diagram for $I=2$, negative magnetic moment.

Stroke *et al.*[9] in measuring the anomalies in the long-lived radioisotopes Cs^{134}, Cs^{135}, and Cs^{137}.

Because of experience at Berkeley in detecting radioactive beams by counting the activity deposited on a collecting surface at the focus of the apparatus,[10] a beam machine has been constructed to measure the $\Delta\nu$ and g_I of the shorter-lived radioactive alkalis with sufficient precision to obtain a measure of possible hfs anomalies. We have developed a technique for measuring the nuclear moment without sacrificing so much intensity as to make detection by deposition impractical, as would be the case if one attempted the technique of Eisinger, where $\Delta F=0$ transitions are focused by operating the deflecting magnets in the intermediate field region. Although some precision is sacrificed, a usable value of the anomaly can be obtained. After checking the technique by measurement of these constants on stable Rb^{85} and comparing them with results previously published by other workers, we have measured the $\Delta\nu$ and g_I of 18.6-day Rb^{86}, calculated the Rb^{85}-Rb^{86} hfs anomaly, and made a comparison with values predicted by using various nuclear models and the Bohr-Weisskopf theory.

II. THEORY OF THE EXPERIMENT

The Hamiltonian of an atom with a $J=\frac{1}{2}$ electronic ground state in an external magnetic field H_0 is given by

$$\mathcal{H}=ha\mathbf{I}\cdot\mathbf{J}-g_J\mu_0\mathbf{J}\cdot\mathbf{H}_0-g_I\mu_0\mathbf{I}\cdot\mathbf{H}_0, \quad (7)$$

where I is the nuclear spin and a is the hfs splitting factor. When H_0 is zero, the two F levels ($\mathbf{F}=\mathbf{I}+\mathbf{J}$) are separated by $\Delta\nu$. As H_0 is increased, the $(2F+1)$-fold degeneracy of each level is split and the eigenvalues of the Hamiltonian in the (F,m_F) representation are given by the Breit-Rabi equation[11]

$$W(F,m_F)=-\frac{h\Delta\nu}{2(2I+1)}-g_I\mu_0H_0m_F \pm\frac{h\Delta\nu}{2}\left[1+\frac{4m_F}{2I+1}x+x^2\right]^{\frac{1}{2}}, \quad (8)$$

where the dimensionless parameter x has the form

$$x=(g_I-g_J)\mu_0H_0/h\Delta\nu, \quad (9)$$

with the convention that g_J for alkalis has a negative sign. The positive sign before the square root in Eq. (8) refers to the state $F=I+\frac{1}{2}$ and the negative sign to the state $F=I-\frac{1}{2}$. The Breit-Rabi energy level diagram for $I=2$ and a negative g_I is shown in Fig. 1.

A collimated beam of neutral atoms is directed through a series of three magnets; the first (A magnet) has a field gradient transverse to the beam; the third (B magnet) is identical to the first and has its gradient in the same direction. The second (C magnet) is a homogeneous field containing a "hairpin" capable of introducing an oscillating rf field in the beam region. While in the inhomogeneous field, the atom experiences a transverse force

$$F=\mu_{\text{eff}}\nabla H,$$

where

$$\mu_{\text{eff}}=-\partial W/\partial H$$

is the effective magnetic moment. In the "flop-in" method used in this experiment, an atom must undergo a transition in the C field which changes the sign of μ_{eff} in order to be refocused at the detector located on the beam axis, since the deflection in the third magnet must be equal and opposite to that in the first. The deflecting fields are operated at several thousand gauss, so that I and J are decoupled and only $\Delta m_J=\pm1$ transitions are focusable in our apparatus. The magnetic dipole selection rules

$\Delta F=0,\ \pm1,\ \Delta m_F=0$ for σ transitions, $H_{\text{rf}}\|$ to H_0,

$\Delta F=0,\ \pm1,\ \Delta m_F=\pm1$ for π transitions, $H_{\text{rf}}\perp$ to H_0,

apply to transitions induced by the oscillating rf field.

Observation of field independent transitions are required to obtain the narrow lines necessary for precision measurements. In the Zeeman region of hyperfine structure there is a transition which is field independent to second order with a value very close to $\Delta\nu$. For isotopes of half odd-integer spin this is a singlet σ transition, and for those of integer spin it is a doublet π transition. By exciting π transitions with a strap hairpin approximately

[9] H. H. Stroke, V. Jaccarino, D. S. Edmonds, and R. Weiss, Phys. Rev. **105**, 590 (1957).

[10] See, for example, W. A. Nierenberg, Ann. Rev. Nuclear Sci. **7**, 349 (1957).

[11] G. Breit and I. I. Rabi, Phys. Rev. **38**, 2082 (1931).

2 cm long, $\Delta\nu$ for Rb^{86} can be determined to within a few kc. Details of the transition calculation appear in the Appendix.

In the intermediate field region, for isotopes with $I \geqslant 1$, the $\Delta F = \pm 1\,\pi$ doublet involving the levels $(F^+, \mp F^+ \pm 2) \leftrightarrow (F^-, \mp F^-)$ and $(F^+, \mp F^+ \pm 1) \leftrightarrow (F^-, \mp F^- \pm 1)$,[12] has a separation $2g_I\mu_0 H_0/h$, and its mean value passes through a minimum so that the transitions are insensitive to variations of field in this region. The value of the parameter at which this minimum frequency occurs is a function only of the spin I; the frequency at that point is a function only of I and $\Delta\nu$. Details of these transitions for the two isotopes of interest here are given in the Appendix. If these transition frequencies can be measured accurately enough, both g_I and $\Delta\nu$ can be obtained and the anomaly calculated if these constants are known for the other isotope. From Eq. (5) the anomaly is given by

$$ {}^1\Delta^2 = \left[\frac{(\Delta\nu)_1}{(\Delta\nu)_2}\left(\frac{2I_2+1}{2I_1+1}\right)\frac{g_{I_2}}{g_{I_1}}\right] - 1, \qquad (10) $$

where, by convention,[5] isotope 1 is the lighter of the two.

III. APPARATUS

The atomic-beam apparatus used in the experiment has been constructed for the purpose of measuring hfs anomalies of radioactive alkalis and is described below. The vacuum tank and magnets of a molecular beam apparatus built by Bemski[13] were used with new lower gradient pole faces for the deflecting magnets.

A. Geometry and Vacuum System

The deflecting magnets are arranged to detect transitions by the "flop-in" method, so that a refocused beam causes an increase over the background in the detector signal.

The vacuum tank is $78\frac{5}{8}$ in. long, 12 in. i.d., and is rolled from $\frac{1}{4}$-in. stainless steel sheet. Two brass bulkheads separate the tank into three sections: oven, buffer, and main chamber, each pumped separately by oil diffusion pumps. Operating pressures are 10^{-6} mm Hg in the main chamber and 10^{-5} to 10^{-6} mm Hg in the oven chamber. O-ring seals are used throughout, both for static seals of cover plates and sliding seals for beam flag, stop wire, and detector motions. A stop wire is placed on the beam axis in the center of the B magnet to prevent the very fast undeflected atoms from the tail of the Boltzmann distribution from contributing to the detector background. A collimator slit is placed at the center of the C magnet.

The oven for production of a rubidium beam is made from a stainless steel block $\frac{7}{8}$ in. $\times 1$ in. $\times \frac{5}{8}$ in. The beam material is placed in a $\frac{7}{16}$-in. diam cylindrical cavity in the block closed by a press fit cap. Stainless steel slit jaws $\frac{1}{8}$ in. thick are screwed to the oven body; a slit width of 0.005 in. was found to give satisfactory operation and no further channeling was utilized. The oven was heated to about 500°C by bombardment of electrons emitted from a U-shaped tungsten filament of 0.020-in. diam positioned in the vertical plane $\frac{1}{8}$ in. in front of the slit. Between 10 and 50 watts power is required for a usable beam.

For work with materials of short half-life, it is necessary to provide a means of placing the oven in position inside the vacuum without waiting for the machine to be pumped down to its operating condition from atmospheric pressure. A vacuum lock arrangement is provided which allows an oven to be inserted in a few minutes.

B. Magnets

The A and B magnets are identical low-impedance electromagnets operated at 300 amp from a bank of submarine batteries.

The C magnet is also a low-impedance electromagnet having a gap 0.250 in. wide and $15\frac{5}{8}$ in. long. By utilizing the presence of the stable carrier isotope in the beam, the field of this magnet can be stabilized at any desired value by electronically locking to the peak of some suitable resonance of the carrier isotope. Details of this system have been described elsewhere.[14] Field stability depends on the linewidth of the resonance used; typical values are ± 0.02 gauss at 3 gauss and ± 0.1 gauss at 600 gauss.

C. Detectors

Surface ionization detectors consisting of heated K-free tungsten ribbons and an ion collector plate are used to detect the stable alkali beam. The radioactive component is detected by allowing the beam to fall on the sulfur surface of a brass "button" which can be inserted and removed through vacuum locks at the focus of the machine. The collected activity is then counted on low-background NaI(Tl) scintillation counters.

One ionization detector, a 0.010-in. tungsten ribbon mounted in the center of the 0.065-in. exit slit, is used to detect the resonance used for locking the C field. Another, a 0.075-in. ribbon, is placed in one position of the rotary button loader which contains two button locks and a window in the other 3 positions and is used to detect the field calibrating resonance.

The pattern of the deflected beam in the focal plane normal to the beam direction is symmetrical about the focus and shows as a single well-defined peak (for $J = \frac{1}{2}$). If the width of the undeflected beam is much less than the deflection, S_m, of the peak, it can be shown[15] that

$$ S_m \simeq \tfrac{1}{3} S_\alpha, $$

[12] Here $F^\pm = I \pm \frac{1}{2}$ and the upper signs are applicable for positive g_I, the lower ones for negative g_I.

[13] G. Bemski, Thesis, University of California, 1953 (unpublished).

[14] G. O. Brink and N. Braslau, Rev. Sci. Instr. **30**, 670 (1959).

[15] N. F. Ramsey, *Molecular Beams* (Oxford University Press, New York, 1956), p. 99.

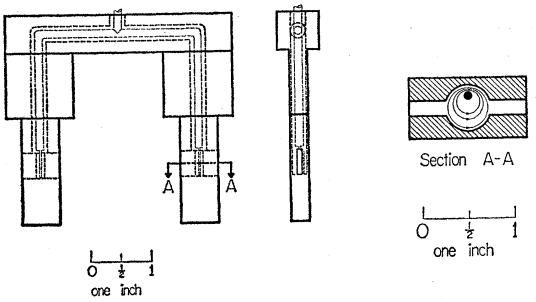

FIG. 2. Hairpin for inducing separated oscillatory fields. Section A-A is taken along the beam path and indicates the radio-frequency magnetic field lines in the *TEM* mode.

where S_α is the deflection of an atom with the most probable velocity, $\alpha=(2kT/m)^{\frac{1}{2}}$, in the oven. For a symmetrical apparatus where the A and B fields are identical and operated at a field H,

$$S_\alpha=KH/kT,$$

where K is a constant taking into account the geometry of the apparatus and the properties of the magnets. The intensity of the deflected beam at the peak can be shown to be a function only of S_α and the total rate of effusion from the oven. For small changes in oven temperature and magnitude of deflecting fields (as during a run), the beam intensity at the deflected peak is a function only of the oven effusion rate and serves as a convenient means of monitoring any changes in the beam intensity during a run. A third ionization detector, located to one side in front of the plane of the exit slit, monitors the intensity of the deflected peak and serves to normalize the exposed buttons to a constant beam level. The output of these ionization detectors is read by a Beckman model 5 vibrating-capacitor electrometer.

D. Production of the Beam

The isotope Rb^{86} is obtained from Oak Ridge National Laboratory in the form of RbCl in a weak HCl solution, in shipments of 300 millicuries with specific activities ranging from 300 mC/g to 12 000 mC/g. Where possible, specific activity was reduced to approximately 2000 mC/g for these runs. The solution was evaporated to dryness using hot nitrogen gas, and the RbCl powder was placed in the oven with freshly filed calcium chips. Reduction of the chloride took place at about 10 w of electron bombardment power, and a beam level of 2 to 3×10^{-10} amp of ion current was observed by the detector placed in the exit slit; this beam level was maintained throughout the run with a typical load of about 150 mg lasting six hours.

E. Radio-Frequency System

Button exposure times of 5–20 min require the rf oscillators to have long-time stability of the order of 1 part in 10^7. The heart of the assembled system is a Gertsch AM-1 20–40 Mc/sec phase locked oscillator and a Gertsch FM-4 500–1000 Mc/sec oscillator locked to a harmonic of the output of the AM-1. A 100-kc/sec standard frequency is provided for the AM-1 and is also used to generate the time base for a Hewlett-Packard HP524B frequency counter. The 100 kc/sec is furnished by a James Knights JKFS 1100 secondary frequency standard which has been determined to drift less than 1 part in 10^9 per week, by comparison with the laboratory's National Company Atomicron, a cesium-beam primary frequency standard.

With continuous monitoring by the frequency counter of the 1–2 Mc/sec free-running oscillator in the AM-1 which is mixed with integral megacycle harmonics of the 100-kc/sec input in that instrument, outputs stable to 1 part in 10^7 are obtained. Frequencies above 1000 Mc/sec are obtained by taking a harmonic of a suitable frequency in the range 500–1000 Mc/sec. After filtering, the signal is amplified by one of a series of traveling-wave tube amplifiers and then carried to the hairpin by coaxial line. A second set of Gertsch oscillators is provided to furnish a frequency-modulated output for locking the C magnet.

For preliminary work and for calibration of the C field by observation of some field-dependent line of the stable carrier isotope, conventional signal generators, such as the Hewlett-Packard 608A and Tektronix 190, are used with suitable amplifiers.

Copper strap hairpins $\frac{3}{4}$-in. wide were used to induce the field locking transition, and for observing the $\Delta F=0$ flop-in transition and the $\Delta F=1$ Zeeman lines in both the stable and radioactive isotopes. For observation of the intermediate field doublet, a hairpin providing in-phase separated oscillatory fields was used to induce the transition, giving rise to the characteristic Ramsey patterns.[16] This hairpin consists of parallel sections of coaxial line with a transition to an eccentric coaxial line in the beam region where each arm is shorted directly below the beam path. Figure 2 is a drawing of the structure and shows the rf field lines in the *TEM* mode in the beam region. Only the region where the lines are parallel to the beam is effective in inducing the π transitions; the oscillating field intensity is not a step function along the beam, but approximates a condition considered by Ramsey—that of a step function with wings,[17] and its effect on the line shape would only narrow slightly the pedestal upon which the interference pattern sits. This hairpin also excites σ transitions because of the two out-of-phase patches of rf at the entrance and exit.[18] The typical out-of-phase Ramsey pattern has been seen on σ transitions of stable isotopes, but is not particularly useful because of its wide linewidth. Since the transition probability on resonance is zero in this case, there is no interference pattern between the two hairpins. The length of the arms of this

[16] Reference 15, p. 124.
[17] N. F. Ramsey, Phys. Rev. **109**, 822 (1958).
[18] This effect has also been observed by G. K. Woodgate and R. W. Hellworth, Proc. Phys. Soc. (London) **A69**, 588 (1956).

TABLE I. Results of observations of the field-independent doublet of Rb^{85}. ν_{87} is the frequency of the $\Delta F=0$ field-calibrating transition of Rb^{87}. Observed frequencies of the components of the doublet are ν^+ and ν^-. The nuclear g factor is calculated using Eq. (20).

Observation	ν_{87} (Mc/sec)	H_0 (gauss)	ν^- (Mc/sec)	ν^+ (Mc/sec)	$\frac{1}{2}(\nu^++\nu^-)$ (Mc/sec)	$\nu^+-\nu^-$ (Mc/sec)	g_I
1	469.41(8)	562.18(8)	2611.6514(3)	2612.1138(3)	2611.8826(5)	0.4624(5)	$2.938(2)\times10^{-4}$
2	469.65(8)	562.41(8)	2611.6512(3)	2612.1136(3)	2611.8824(5)	0.4624(5)	$2.937(2)\times10^{-4}$
3	469.83(8)	562.60(8)	2611.6510(3)	2612.1139(3)	2611.8824(5)	0.4629(5)	$2.939(2)\times10^{-4}$
4	469.95(8)	562.72(8)	2611.6514(3)	2612.1142(3)	2611.8828(5)	0.4628(5)	$2.938(2)\times10^{-4}$
5	470.25(8)	563.03(8)	2611.6515(3)	2612.1145(3)	2611.8830(5)	0.4630(5)	$2.938(2)\times10^{-4}$

structure were chosen to present a 50-ohm input impedance at the connector at 4000 Mc/sec; the separation of the two oscillatory fields is $2\frac{1}{4}$ in., giving a linewidth of 3 kc/sec on the central interference peak. The observed patterns had this width; no shimming of the C magnet was required to observe them.

IV. THE EXPERIMENT

A. Rubidium-85

The hfs separation of stable Rb^{85} was measured by Bederson and Jaccarino from the observation of the field-independent Zeeman line.[19] The moment was measured by Yasaitis and Smaller by NMR.[20] As a check of our method, the intermediate field doublet was observed over a 1-gauss region in the vicinity where its mean value was expected to be a minimum. A typical set of resonances is shown in Fig. 3, as observed on the button loader ionization detector. Results are shown in Table I. For these measurements, the magnetic field was locked to the Rb^{85} $(3,3)\leftrightarrow(2,2)$ transition at 4431 Mc/sec.

In order to check for the presence of a possible phase shift between the two oscillatory fields (which would affect the absolute value of the frequency but not the difference between two frequencies), the hairpin was reversed with respect to the beam direction and the experiments repeated. Within the criterion set for the uncertainty of the peak ($\frac{1}{10}$ the full width at half maximum) no shift was observed; from the symmetry of the patterns none was expected.

The values of the constants were obtained by a best fit to the transition frequencies obtained from the Breit-Rabi equation, using an IBM-704 routine written by W. B. Ewbank of this laboratory using the following values of the physical constants:

$$h=6.62517(23)\times10^{-27}\text{ erg sec},^{21}$$
$$\mu_0=0.92731(2)\times10^{-20}\text{ erg/gauss},$$
$$g_J(\text{Rb})=-2.00238(2).^{22}$$

The results for Rb^{85} are found to be

$$\Delta\nu=3035.7327(7)\text{ Mc/sec},$$
$$g_I=2.938(2)\times10^{-4},$$

to be compared to the previously published values,

$$\Delta\nu=3035.735(2)\text{ Mc/sec},^{19}$$
$$g_I=2.93704(4)\times10^{-4}.^{20}$$

B. Rubidium-86

1. Experimental Procedure

For runs with this radioisotope, the following procedure was used: when the undeflected beam reached a steady value of about 2×10^{-10} amp, a button was exposed to establish the specific activity of the beam. The deflecting fields were turned on and the monitor detector moved to the peak of the flopped-out beam and a reading taken at that point. The C magnet was degaussed and the C magnet current increased until the locking resonance was focused. The field was locked to the peak of this resonance and the calibrating resonance observed. The first search frequency was introduced and a button exposed. At the end of an exposure, the button loader was rotated to the window position, the search frequency changed, and the button loader rotated to the next exposure position, after which the previously exposed button could be removed through a vacuum lock and a fresh one inserted for the next exposure. After several buttons had been exposed, the button loader

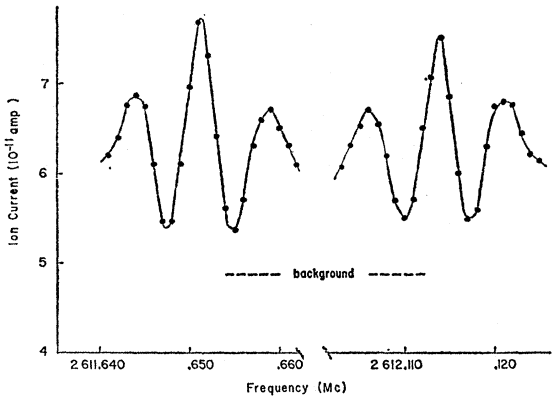

FIG. 3. Typical resonances observed on the field-independent doublet of Rb^{85} using separated oscillatory fields.

[19] B. Bederson and V. Jaccarino, Phys. Rev. **87**, 228 (1952).
[20] E. Yasaitis and B. Smaller, Phys. Rev. **82**, 750 (1951).
[21] E. R. Cohen, K. M. Crowe, and J. W. M. DuMond *The Fundamental Constants of Physics* (Interscience Publishers, New York, 1957).
[22] P. Kusch and H. Taub, Phys. Rev. **75**, 1477 (1949).

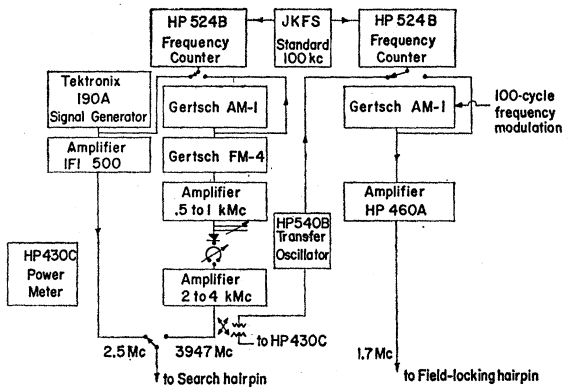

FIG. 4. Arrangement of radiofrequency equipment for measuring $\Delta F=1$ Zeeman transitions in Rb^{86}.

was rotated to place the ionization detector in the focus and the calibrating resonance was again observed to check the field lock. At the end of a run the monitor detector was read, the deflecting magnets turned off, and the undeflected beam level read again as a check of the monitor calibration. The exposed buttons were then counted, background subtracted, and correction made for beam normalization. Individual button counting rates were plotted against their exposure frequency and the resonance curve was fitted both by eye and by an IBM-650 computer routine written by H. B. Silsbee, which fits a bell-shaped curve to the data by the method of least squares.

2. *Measurements*

By observation of the $F=I+\frac{1}{2}$, $m_F=-(I+\frac{1}{2})\leftrightarrow -(I-\frac{1}{2})$ transition at several values of static field in the range 4–163 gauss, Bellamy and Smith determined that $I=2$, $g_I=-1.7$ nm, and $\Delta\nu=3960\pm20$ Mc/sec.[23,24]

TABLE II. Results of the measurement of the Rb^{86} hfs separation. Runs 33–79 were made in the Zeeman region, where $\Delta\nu$ was calculated using Eq. (26). The mean frequency $\bar{\nu}$ of the intermediate field doublet was used to calculate $\Delta\nu$, the relationship being given by Eq. 23.

($m_F=\pm\frac{1}{2}\leftrightarrow m_F=\mp\frac{1}{2}$ Zeeman transition)

Run	ν (Mc/sec)	$\nu(Rb^{87})$ (Mc/sec)	$\Delta\nu$ (Mc/sec)	Remarks
33	3946.891(5)	1.52	3946.886(5)	$\frac{3}{4}$-in. strap
39	3946.900(4)	2.98	3946.883(4)	$1\frac{1}{4}$-in. strap
	3946.893(4)	2.37	3946.882(4)	
	3946.887(4)	1.66	3946.882(4)	
63	3946.894(4)	2.24	3946.884(3)	2-in. strap
78	3946.898(4)	2.66	3946.884(3)	
79	3946.894(4)	2.28	3946.884(3)	

Intermediate-field doublet

Hairpin position	$\bar{\nu}$ (Mc/sec)	Average $\bar{\nu}$ (Mc/sec)	$\Delta\nu$ (Mc/sec)
Original run 92	3599.9340(5)	3599.9345(8)	3946.883(1)
Reversed run 100	3599.9350(5)		

[23] E. H. Bellamy, Nature **168**, 556 (1951).
[24] E. H. Bellamy and K. F. Smith, Phil. Mag. **44**, 33 (1953).

This transition was then observed by us in fields up to 630 gauss. At this field the peak of the transition occured at 516.6±0.1 Mc/sec, leading to $\Delta\nu=3948.7\pm2.0$ Mc/sec.

It was then feasible to search for $\Delta F=1$ transitions in a field of 3 gauss. The four-π transitions were seen, and several observations of the field-independent line made, with different hairpins at various values of the static magnetic field. The rf system for these experiments is shown in Fig. 4. The field was locked to the $\Delta F=0$ refocusable transition in Rb^{85} and calibration was made with the $\Delta F=0$ transition in Rb^{87}. The results are given in Table II.

The position of the components of the field-independent doublet could then be predicted to within a few linewidths, details of which are given in the Appendix. At a field of 591.9 gauss, with the magnet locked to the $(3,3)\leftrightarrow(2,2)$ transition in Rb^{85} at 4508 Mc/sec, where the $\Delta F=0$ Rb^{85} calibrating resonance was at 457.5 Mc/sec, the search for these lines was made with the separated oscillatory field hairpin. The rf block diagram for this stage of the experiment is shown in Fig. 5. A typical set of Ramsey patterns observed on these lines is shown in Fig. 6. The persistent asymmetry of the line indicated that there was a phase shift at this frequency and, upon reversing the hairpin, it was found that the absolute frequency of the lines did shift, but that the separation was unchanged and that the separation of the doublet in each position was the same as the separation of the average value of the two lines in the two positions. This is consistent with the assumption that there is a phase-shift distortion, probably due to the presence of polystyrene supporting beads in the coaxial structure, which shifts the peak of the resonance but has the same value for the two lines since their separation is small compared with the frequency. The actual value of the transition frequency can be found from the mean value of the transitions in the two hairpin positions. If the phase shift was due to a difference in physical length of the two arms, it would have been observable on the transitions seen in Rb^{85}.

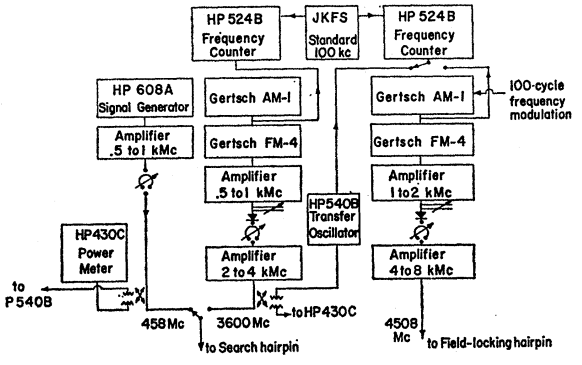

FIG. 5. Arrangement of radio-frequency equipment for measuring field-independent doublet transitions in Rb^{86}.

TABLE III. Results of observations of the field-independent doublet of Rb^{86}. Run 100 was made at the same field as run 92, but with the hairpin reversed with respect to the beam direction.

Run	ν^+ (Mc/sec)	ν^- (Mc/sec)	$\nu^+-\nu^-$ (Mc/sec)	H_0 (gauss)	g_I
91	3600.3148(6)	3599.5536(6)	0.7602(9)	591.86(10)	$-4.588(6)\times10^{-4}$
	3600.3142(6)	3599.5536(6)	0.7606(9)	591.86(10)	$-4.591(6)\times10^{-4}$
92	3600.3143(3)	3599.5537(3)	0.7606(5)	591.87(10)	$-4.593(3)\times10^{-4}$
93	3600.3142(3)	3599.5537(3)	0.7605(5)	591.70(10)	$-4.591(3)\times10^{-4}$
100[a]	3600.3152(3)	3599.5547(3)	0.7605(5)	592.02(10)	$-4.589(3)\times10^{-4}$
	$\bar{\nu}^+$ (Mc/sec)	$\bar{\nu}^-$ (Mc/sec)	$\bar{\nu}^+-\bar{\nu}^-$	H_0 (gauss)	g_I
92–100[a]	3600.3147(5)	3599.5542(5)	0.7605(7)	591.9(2)	$-4.590(4)\times10^{-4}$

[a] Indicates hairpin in reversed position. The average values above are averages of each transition for the hairpin structure in both positions.

The observations on this doublet are summarized in Table III.

The results are, for Rb^{86} in the $^2S_{\frac{1}{2}}$ state,

$$\Delta\nu = 3946.883(2) \text{ Mc/sec},$$
$$g_I = -4.590(4)\times10^{-4},$$
$$\mu_I = Ig_I(M_p/M_e) = -1.6856(14) \text{ nm},$$

where the diamagnetic correction to the moment is not included, and, using the corresponding values of Rb^{85}, for the isotopes Rb^{85}-Rb^{86},

$$\frac{a_1}{a_2}=\frac{\Delta\nu_1}{\Delta\nu_2}\left(\frac{2I_2+1}{2I_1+1}\right)=0.6409562(6),$$

$$g_{I1}/g_{I2}=0.63988(56),$$

giving from Eq. (10)

$$^{85}\Delta^{86}=0.17(9)\%.$$

V. PREDICTION OF THE ANOMALY

A. Theory of the Anomaly

The Bohr-Weisskopf theory considers the nuclear magnetism to be made of a spin and an orbital contribution[2]: the former caused by the distribution of particles throughout the nucleus, each of which possesses an intrinsic spin angular momentum and magnetic moment; the latter due to circulating currents in the nucleus caused by the movement of charged nucleons. This finite volume effect is important only for electronic s states in which the density of the electronic wave function at the nucleus is large. It is very small for $p_{\frac{1}{2}}$ states and negligible for states of higher J.

The fractional reduction ϵ of the hfs separation for a given isotope is[5]

$$\epsilon = -(\bar{K}_s\alpha_s+\bar{K}_l\alpha_l), \tag{11}$$

where α_s and α_l are the respective fractions of the nuclear magnetism that are due to spin and orbital angular momentum, and $\bar{K}_s$ and $\bar{K}_l$ are the averages of K_s and K_l over the nuclear radial coordinate, where

$$K_s=\int_0^R\left[1+\zeta\frac{r}{R}\right]^3 FGdr \Big/ \int_0^\infty FGdr,$$

$$K_l=\int_0^R\left[1-\frac{r}{R}\right]^3 FGdr \Big/ \int_0^\infty FGdr.$$

F and G are the Dirac radial wave functions of the electron, R is the nuclear radial coordinate, r is the electron radial coordinate, and ζ takes into account the angular asymmetry of the spin distribution.[4] It depends

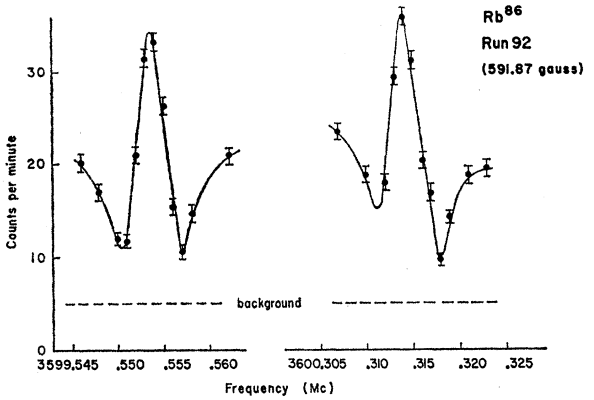

FIG. 6. Typical resonances observed on the field-independent doublet of Rb^{86} using separated oscillatory fields.

on the particular nuclear model chosen. In particular, for the single-particle model, Bohr finds

$$\zeta=(2I-1)/4(I+1) \quad \text{for} \quad I=l+\tfrac{1}{2},$$
$$\zeta=(2I+3)/4I \quad \text{for} \quad I=l-\tfrac{1}{2}.$$

The integral above may be evaluated by writing F and G as a power series in r/R inside a uniformly charged sphere of radius R_0 and matching these functions at the nuclear radius R_0 with the standard solutions for an unscreened Coulomb potential.[25] In their original paper,[2] Bohr and Weisskopf included only terms in the expansion to $(R/R_0)^2$, approximating the contributions of

[25] J. E. Rosenthal and G. Breit, Phys. Rev. 41, 459 (1932).

higher order terms. Their result is

$$\epsilon=-[(1+0.38\zeta)\alpha_s+0.62\alpha_l]b\langle(R/R_0)^2\rangle_{\rm av}, \quad (12)$$

where b is a function of R_0 and Z, the nuclear charge, and is tabulated in reference 2. Note that the value $r_0=1.5\times10^{-13}$ cm was used in this paper in the expression for the nuclear radius, $R_0=r_0A^{\frac{1}{3}}$, instead of the more recent value of $r_0=1.2\times10^{-13}$ cm.[26]

Eisinger and Jaccarino[5] have extended this calculation to include terms in $(R/R_0)^4$, with the results

$$\begin{aligned}K_s&=(b_{s2}+b_{s2}')\langle(R/R_0)^2\rangle_{\rm av}-(b_{s4}+b_{s4}')\langle(R/R_0)^4\rangle_{\rm av},\\ K_l&=b_{l2}(R/R_0)^2-b_{l4}(R/R_0)^4,\end{aligned} \quad (13)$$

with the constants b tabulated for $10\leqslant Z\leqslant90$.

It is necessary to make some assumptions about the particle distribution in the nucleus in order to evaluate the averages over the nuclear radial coordinate. As a compromise between the value 1 for a surface distribution and $\frac{3}{5}$ for a volume distribution, Bohr and Weisskopf assumed $(R/R_0)^2=0.8$. Eisinger and Jaccarino assumed a single-particle model in which the odd nucleon moves in a spherically symmetric square-well potential. Their calculations for these averages are presented in the form of graphs in reference 5.

There remains the problem of determining the fractional contributions α_s and α_l. If the nuclear g factor is defined by the equation

$$g_I\mathbf{I}=g_s\mathbf{S}+g_l\mathbf{L} \quad (14)$$

the fractional contributions are given by

$$\begin{aligned}\alpha_s&=\frac{g_s}{g_I}\frac{(g_I-g_l)}{(g_s-g_l)},\\ \alpha_l&=1-\alpha_s=\frac{g_l}{g_I}\frac{(g_I-g_s)}{(g_s-g_l)}.\end{aligned} \quad (15)$$

If the spin and orbital angular momenta can be expressed in terms of $\mathbf{S}$ and $\mathbf{L}$, respectively, for the particular model, α_s and α_l are known and ϵ can be found. From Eq. (6), a value of the anomaly can be calculated for two isotopes.

Since the nucleus is not a point charge, the electrostatic potential in the neighborhood of the nucleus deviates from the pure Coulomb potential. The charge distribution for two isotopes generally is different and affects the ratio of the hfs interactions. This is known as the Breit-Rosenthal effect. Theoretical estimates[27] indicate that the contribution to Δ is of the order of 0.01%, which is negligible in this work but may in some cases exceed the Bohr-Weisskopf effect.[28] Stroke has recently extended the results of Eisinger and Jaccarino to include the effects of the charge distribution which enter into the evaluation of the coefficients b in Eq. (13), so that the Breit-Rosenthal effect can be included in the framework of the Bohr-Weisskopf theory.[6]

The reduced-mass correction to the electron wave function is $(1+m/Am)^{-3}$, which, for two isotopes of different mass, gives an isotope-shift correction to Δ that is important only for the very light elements.

The presence of neighboring fine-structure levels will, in second order, perturb levels of the same F and modify the hfs interaction. The effect on $P_{\frac{1}{2}}$ electrons by the closely lying $P_{\frac{3}{2}}$ level—which has been treated by Clendenin[29]—affects the ratio of the g_I's in the $P_{\frac{1}{2}}$ state. For $S_{\frac{1}{2}}$ states considered in this work, this effect should be negligible; the second-order perturbation effect is of the order of $(\Delta\nu)^2/\delta$, where δ is the separation of the s state and the next state of even parity. For rubidium this is less than 10^{-4}% and is negligible.

B. Nuclear Models of Odd-Proton Odd-Neutron Isotopes

1. Single-Particle Model

The simplest particle description of an odd-odd nucleus is to attribute the nuclear properties to the odd proton and odd neutron, each in its appropriate shell model state,[30] with the total angular momentum of these two particles vector-coupled to give the g factor

$$g_I=\frac{\mathbf{I}_p\cdot\mathbf{I}}{I(I+1)}g_p+\frac{\mathbf{I}_n\cdot\mathbf{I}}{I(I+1)}g_n, \quad (16)$$

where I is the spin of the isotope, I_p and I_n the total angular momentum of the proton and neutron, respectively, g_p and g_n the proton and neutron g factor, which are given for either nucleon by

$$g=\frac{\mathbf{s}\cdot\mathbf{j}}{j(j+1)}g_s+\frac{\mathbf{l}\cdot\mathbf{j}}{j(j+1)}g_l,$$

where j is the nucleon's total angular momentum and g_s and g_l are the spin and orbital g factors of the "free" nucleon, as follows:

Proton	Neutron
$g_l=1$	$g_l=0$
$g_s=5.59$	$g_s=-3.83$.

Note that in this section, for computational convenience, magnetic moments are given in units of nuclear magnetons.

Nordheim pointed out that the ground-state spin of a number of odd-odd nuclei could be accounted for on the basis of this model, plus empirical rules giving the coupling of the odd nucleons.[31] These rules can be

[26] K. W. Ford and D. L. Hill, Ann. Rev. Nuclear Sci. **5**, 25 (1955).
[27] M. F. Crawford and A. L. Shawlow, Phys. Rev. **76**, 1310 (1949).
[28] Y. Ting and H. Lew, Phys. Rev. **105**, 581 (1957).
[29] W. W. Clendenin, Phys. Rev. **94**, 1590 (1954).
[30] M. Mayer and J. H. D. Jensen, *Elementary Theory of Nuclear Shell Structure* (John Wiley & Sons, New York, 1955).
[31] L. W. Nordheim, Phys. Rev. **78**, 294 (1950).

justified on the assumption that the intrinsic spins of these two odd particles always tend to line up parallel. The rules are:

"strong" rule:

$$I=|j_p-j_n|, \quad \text{if} \quad j_p=l_p\pm\tfrac{1}{2} \quad \text{and} \quad j_n=l\mp\tfrac{1}{2},$$

"weak" rule:

$$|j_p-j_n|<I\leq j_p+j_n, \quad \text{if} \quad j_p=l_p\pm\tfrac{1}{2} \quad \text{and} \quad j_n=l_n\pm\tfrac{1}{2}.$$

Fair agreement with experiment can be obtained for magnetic moments by using this model, but although the approximate agreement is encouraging, the model is not sophisticated enough for one to hope to account for the moments of heavier nuclei. It should be pointed out that the above equations are equally valid for a proton or neutron "hole" in a closed angular momentum shell.

For nuclei in which the neutron and proton states are different, Schwartz suggested that Eq. (16) should still be used, but that the g_p and g_n should represent empirical g factors of the odd-A nuclei $(Z, N-1)$ and $(Z-1, N)$ respectively, where Z and N are the proton and neutron numbers of the particular odd-odd nucleus.[32] This rule is more successful than using free-particle g factors. Unfortunately, these empirical g factors are not always known, but Schwartz finds that using those of nearby nuclei in the same state gives reasonable agreement.

2. Collective Model

Bohr and Mottelson[33] consider a system of a single particle and a distorted core which is assumed to be uniformly charged and have a g factor

$$g_R\simeq Z/A.$$

For the case where the total j of the odd particle is coupled to this core,

$$g_I=g_\Omega[I/(I+1)]+g_R[1/(I+1)],$$

where Ω is the projection of j along the nuclear symmetry axis; for the ground state, $I=\Omega$.

Generalizing to two particles, one finds

$$g_\Omega=(1/\Omega)[\Omega_n g_\Omega(n)+\Omega_p g_\Omega(p)],$$

where $g_\Omega(n)$ and $g_\Omega(p)$ are the g factors in an ellipsoidal potential. Since these are not usually known, g values for pure j states are used; agreement with experiment is expected to be poor. For nuclei with odd particles close to closed shells, such as Rb^{86}, the core is expected to be close to spherical and the model is not expected to be useful.

Gallagher and Moszkowski have determined general coupling rules analogous to Nordheim rules above, making the assumption that the components of the neutron and proton spin along the nuclear symmetry axis always couple parallel.[34]

[32] H. M. Schwartz, Phys. Rev. **89**, 1293 (1953).
[33] A. Bohr and B. R. Mottelson, Kgl. Danske Videnskab. Selskab, Mat.-fys. Medd. **27**, 16 (1953).

TABLE IV. The nuclear moment of Rb^{86} as predicted by various nuclear models. The first single-particle (SP) model prediction is made using "free" nucleon g factors in Eq. (16). The second uses the measured g factors of nearby odd-A nuclei in the same single-particle states as the odd proton and odd neutron.

μ_{exp}	SP, g(free)	SP, g(emp)	Collective[33]	Collective[34]	Config.[36] mixing
−1.686	−2.13	−1.7	−1.56	−1.14	−1.0

3. Configuration Mixing Model

For odd-A nuclei, attempts to account for the deviation of the measured magnetic moments from the Schmidt limits have required the mixing of different nucleon configurations with the odd single-particle configuration[35] due to very-short-range internucleon forces. This mixing is assumed to be small, but can profoundly affect the expectation value of the magnetic-moment operator. This theory has been quite successful in predicting moments of odd-A nuclei.

Recently the theory has been extended to include odd-odd nuclei,[36] but the agreement of the calculated moments with experiment has not been very satisfactory. Predicted values of the nuclear magnetic moment of Rb^{86} using these models are given in Table IV.

C. Application of Models to Bohr-Weisskopf Theory

Two models are considered in calculating the anomaly, both of which are of the single-particle type. In model 1, the difference between the observed g value and the Schmidt value is eliminated by a reduction of the spin moment of the odd nucleon, which may be considered to be caused by exchange currents in the nucleus. In model 2, g_l instead of g_s is modified to give the observed value.[37] To give a predicted Δ for Rb^{85}-Rb^{86}, each model is applied to three stages of the Bohr-Weisskopf theory: (a) the original theory as modified by Bohr; (b) the extension by Eisinger and Jaccarino; (c) the extension by Stroke to include effects of the charge distribution.

D. Predictions of the Rb^{85}-Rb^{86} hfs Anomaly

Model 1. For one odd nucleon in a single-particle state, the g factor is given by Eq. (17). For Rb^{85} the odd proton is in a $f_{\frac{5}{2}}$ state, and one finds, assuming g_l(proton) $=1$, g_l(neutron) $=0$,

$$g=-(1/7)g_s^{\text{eff}}+8/7.$$

[34] C. G. Gallagher and S. A. Moszkowski, Phys. Rev. **111**, 1282 (1958).
[35] A. Arima and H. Horie, Progr. Theoret. Phys. (Kyoto) **12**, 623 (1954).
[36] H. Noya, A. Arima, and H. Horie, Progr. Theoret. Phys. (Kyoto) Suppl. **8**, 33 (1958).
[37] F. Bloch, Phys. Rev. **83**, 839 (1951).

Using the empirical value of g for Rb^{85} (0.539), one finds $g_s^{\text{eff}}=4.22$. Then $\alpha_s=-1/7g_s^{\text{eff}}=-1.114$ and $\alpha_l=(1-\alpha_s)=2.114$.

For Rb^{86} the g factor is given by Eq. (16). It is assumed that the addition of the odd neutron does not affect the proton state, so for g_p the value $g_{\text{exp}}(Rb^{85})$ is used. With $I_p=\frac{5}{2}$ and $I_n=9/2$, Eq. (16) gives $g_n=-0.215$, using the experimental g factor of Rb^{86}. From Eq. (17) with $g_l(\text{neutron})=0$, one finds $g_{sn}^{\text{eff}}=-1.94$. Using these values in Eq. (16) one obtains

$$f=(5/6)g_p+(11/6)(g_{sn}^{\text{eff}}/9),$$

and $\alpha_{sp}=-(5/6)\alpha_s(Rb^{85})$, $\alpha_{lp}=-(5/6)\alpha_l(Rb^{85})$, and $\alpha_{sn}=(11/6)(1/g)(g_{sn}^{\text{eff}}/9)$, giving values 0.928, −1.762, and 0.466, respectively.

Model 1(a). With the fractional contributions obtained above, ϵ is calculated with Eq. (12) as derived by Bohr. For Rb, $b=0.58$, and for the $f_{\frac{5}{2}}$ proton $(R/R_0)^2\simeq 0.8$, and $\zeta=4/5$. For the $g_{9/2}$ neutron, $\zeta=4/11$, $(R/R_0)^2\simeq 0.9$ and the ϵ's are summed for the two odd particles in Rb^{86}.

Model 1(b). Using Eisinger and Jaccarino's equations for a uniform charge distribution, ϵ is calculated from Eq. (11), using $\bar{K}_l$ and $\bar{K}_s$ calculated from Eq. (13). From these authors' tables, for the $g_{9/2}$ neutron, $\mathfrak{R}_{e2}=0.89$ and $\mathfrak{R}_{e4}=0.88$, for the $f_{\frac{5}{2}}$ proton, $\mathfrak{R}_{e2}=0.77$, $\mathfrak{R}_{e4}=0.70$, and the b coefficients for $Z=37$ are used.

Model 1(c). The b's calculated by Stoke for a surface charge distribution[6] are used in Eq. (13). The $\mathfrak{R}_{ei}$ are the same as for model 1(b).

Model 2. Instead of obtaining g_s^{eff}, one modifies g_l to obtain $g(\text{exp})$ for Rb^{85}. As before,

$$g=-(1/7)g_s+(8/7)g_l^{\text{eff}},$$

where $g_l^{\text{eff}}=1.117$. One finds $\alpha_s=-1.46$ and $\alpha_l=2.46$. For Rb^{86},

$$g=-(5/6)g_p+(11/6)g_n,$$

which yields $g_n=-0.216$. Using Eq. (17) (where now the neutron has an "effective" g_l), one finds $g_{ln}^{\text{eff}}=0.119$; g_{sp} and g_{sn} have their "free" nucleon values and $g_{lp}=g_l^{\text{eff}}(Rb^{85})$; then $\alpha_{sp}=-(5/6)\alpha_s(Rb^{85})$, $\alpha_{lp}=-(5/6)\alpha_l(Rb^{85})$, $\alpha_{ln}=(11/6)[(8/9)g_{ln}^{\text{eff}}/g_n]$, and $\alpha_{sn}=(11/6)[1-(8/9)g_{ln}^{\text{eff}}/g_n)]$, which give the values 1.22, −2.05, −0.905, and 2.72, respectively.

Model 2(a). The fractional contributions calculated for model 2 are used with the parameters given under model 1(a), with ϵ calculated using Eq. (12).

Model 2(b). The parameters of model 1(b) and the fractional contributions of model 2 are used with Eqs. (11) and (13).

Model 2(c). The b coefficients appropriate to the surface charge distribution are used with the fractional contributions of model 2.

Results of calculations from all these models are summarized in Table V and are compared with the expected Rb^{85}-Rb^{86} anomaly.

TABLE V. Predictions of the Rb^{85}-Rb^{86} hfs anomaly using a single-particle model. Model 1 modifies g_s to obtain the observed moments; model 2 modifies g_l to obtain the observed moments. Model (a) uses the original Bohr-Weisskopf theory; model (b) uses the formulation of Eisinger and Jaccarino for a uniform charge distribution; model (c) uses the formulation of Stroke for a surface charge distribution.

	$\epsilon(Rb^{85})$ (%)	$\epsilon(Rb^{86})$ (%)	Δ (%)
Experiment	...	...	0.17(9)
Model 1(a)	0.066	−0.331	0.40
Model 1(b)	0.030	−0.293	0.32
Model 1(c)	0.037	−0.219	0.26
Model 2(a)	0.177	−1.46	1.64
Model 2(b)	0.024	−1.11	1.13
Model 2(c)	0.102	−1.00	1.10

VI. CONCLUSION

Comparison of the experimental value of Δ with predictions of those calculated, using the Bohr-Weisskopf theory and a single-particle model of the nucleus with the spin or orbital g factor of the odd nucleon modified to give the observed nuclear g factor, indicates that the modification of g_l gives poor agreement with experiment. However, the vector coupling model for the odd-odd isotope and reduction of the intrinsic spin g_s factor gives reasonable agreement. At this stage one cannot choose between the uniform and surface charge distributions. This work, together with previous work, indicates that one can at least get order-of-magnitude agreement using the existing theory and a reasonably simple single-particle model.

With three sets of anomalies involving three adjacent isotopes (potassium-39, -40, and -41, rubidium-85, -86, and -87; and cesium-133, -134, and -135) now measured, it should be worthwhile to attempt to extend the theory to include the configuration mixing and collective models of odd-odd nuclei.

The apparatus and technique described for measuring the nuclear g factor are not capable of giving the ultimate accuracy desired for a measurement of the anomaly. A new atomic-beam apparatus under construction in this laboratory will permit g factors to be measured more accurately than with the present machine. The measurements made here do indicate that, to at least 1 part per million, the Breit-Rabi equation accurately represents the energy levels of the hyperfine interaction for rubidium atoms in the $^2S_{\frac{1}{2}}$ electronic ground state.

ACKNOWLEDGMENTS

We wish to thank Professor William A. Nierenberg for his interest in and support of this work. We are indebted to Professor Howard A. Shugart for his advice and helpful discussions, to Mr. J. D. Faust for assistance in making the measurements and to Dr. W. B. Ewbank for his critical reading of the manuscript.

APPENDIX

All transitions of interest are of the type $\Delta F=\pm 1$. From Eq. (8) the general equation of a transition

$m_+ \leftrightarrow m_-$ is

$$\nu=\frac{g_I\mu_0 H_0}{h}(m_+-m_-)+\frac{\Delta\nu}{2}\left[\left(1+\frac{4m_+}{2I+1}x+x^2\right)^{\frac{1}{2}}+\left(1+\frac{4m_-}{2I+1}x+x^2\right)^{\frac{1}{2}}\right]. \quad (A.1)$$

A. Rb^{85} Transitions ($I=\frac{5}{2}$)

The doublet of interest for measuring g_I has the m values of $m_+=-1$, $m_-=-2$, and $m_+=-2$, $m_-=-1$. From Eq. (A.1) the mean frequency of this doublet is

$$\bar{\nu}=\tfrac{1}{2}\Delta\nu[(1-\tfrac{2}{3}x+x^2)^{\frac{1}{2}}+(1-\tfrac{4}{3}x+x^2)^{\frac{1}{2}}]. \quad (A.2)$$

The components of the doublet are arranged symmetrically above and below $\bar{\nu}$ and have a separation

$$\nu^+-\nu^-=2g_I\mu_0 H_0/h. \quad (A.3)$$

The value of x for which $\bar{\nu}$ is a minimum is found by differentiating $\bar{\nu}$ with respect to x and setting the derivative to zero. We find

$$x=[11-2(10)^{\frac{1}{2}}]/9=0.519\,493\,84.$$

From Eq. (9), this value of x corresponds to a field of 562.6 gauss. Substituting this value of x in Eq. (A.2),

$$\bar{\nu}=\tfrac{1}{2}\Delta\nu[(0.923\,544\,623)^{\frac{1}{2}}+(0.577\,215\,397)^{\frac{1}{2}}]=0.860\,379\,61\Delta\nu. \quad (A.4)$$

When the transitions have been observed, the value of g_I is obtained by using Eq. (A.3) and $\Delta\nu$ is obtained by using Eq. (A.4) and the minimum observed value of $\bar{\nu}$.

B. Rb^{86} Transitions ($I=2$)

In this case the doublet transition used to measure g_I has the m values $m_+=\frac{3}{2}$, $m_-=\frac{1}{2}$, and $m_+=\frac{1}{2}$, $m_-=\frac{3}{2}$. From Eq. (A.1),

$$\bar{\nu}=\tfrac{1}{2}\Delta\nu\{[1-(6/5)x+x^2]^{\frac{1}{2}}+[1-(2/5)x+x^2]^{\frac{1}{2}}\} \quad (A.5)$$

so that $\bar{\nu}$ is a minimum at

$$x=(14-4\sqrt{6})/10=0.420\,204\,103.$$

Substituting this value of x into Eq. (A.5),

$$\bar{\nu}=\tfrac{1}{2}\Delta\nu[(0.672\,326\,564)^{\frac{1}{2}}+(1.008\,489\,847)^{\frac{1}{2}}]=0.912\,095\,585\Delta\nu. \quad (A.6)$$

Again the components are symmetric above and below $\bar{\nu}$, with a separation $2g_I\mu_0 H_0/h$.

For $x\ll 1$ (Zeeman region) where $\Delta\nu$ must be determined before the doublet search is undertaken, the g_I term in Eq. (A.1) can be neglected, and an expansion of the equation to second order in x yields

$$\nu=\frac{\Delta\nu}{2}\left(2+\frac{2x}{2I+1}(m_+-m_-)+x^2\left[1-\frac{2}{(2I+1)^2}(m_+^2+m_-^2)\right]\right). \quad (A.7)$$

The field-independent line of interest for $I=2$ is an unresolved doublet with the m values $m_+=\pm\frac{1}{2}$, $m_-=\mp\frac{1}{2}$. Substituting these into Eq. (A.7),

$$\nu=\Delta\nu[1+(12/25)x^2]. \quad (A.8)$$

To sufficient accuracy, from Eq. (9),

$$x\simeq 2.8H_0/\Delta\nu,$$

and the $\Delta F=0$ flop-in transition in Rb^{87} is used to calibrate the field, where its frequency is given by

$$\nu_{Rb^{87}}=\frac{2.8H_0}{2(3/2)+1}.$$

Then substituting this into Eq. (A.8) and solving for $\Delta\nu$,

$$\Delta\nu=\nu-0.00194(\nu_{Rb^{87}})^2 \text{ Mc/sec}. \quad (A.9)$$